


# Quantitative spin-dependent electron-electron interaction to calculate the superconducting parameters $\mu$ and $\lambda$

Carl A. Kukkonen <sup>\*</sup>

33841 Mercator Isle, Dana Point, California 92629, USA

 (Received 22 February 2022; revised 20 February 2023; accepted 2 March 2023; published 17 March 2023)

The spin-dependent Kukkonen-Overhauser (KO) effective electron-electron interaction in electron gas with a deformable background is used to calculate the BCS superconducting parameters  $\mu$ ,  $\mu^*$ , and  $\lambda$ . The density and spin local field factors are utilized to incorporate the quantitative effects of exchange and correlation. The repulsive parameter  $\mu$  is compared to results using the historical Thomas-Fermi or nearly equivalent random phase approximation (RPA) interactions. The resulting  $\mu$  using the KO interaction is 45% larger at  $r_s = 1.65$ ; rising to 153% larger at  $r_s = 5.62$ . Retardation reduces the effective repulsion, but  $\mu^*$  is still 20 – 25% larger. The predicted superconducting transition temperature would be reduced by 5 – 20% using the McMillan formula. The attractive superconducting parameter  $\lambda$ , which depends on the electron-test charge interaction and the phonon spectrum, is also calculated using simple Debye-based models for phonon dispersion. This leads to a larger value of  $\lambda$  than the same calculation using Thomas-Fermi or RPA interactions. Modern calculations of the phonon dispersion relations are often done using density functional theory. With the proper exchange and correlation kernel, the self-consistency of the method should yield the correct phonon dispersion relation and electron-phonon matrix elements. If the Thomas-Fermi or RPA interactions are used at any stage, the results for  $\lambda$  are probably quantitatively inaccurate.

DOI: [10.1103/PhysRevB.107.104513](https://doi.org/10.1103/PhysRevB.107.104513)

## I. INTRODUCTION

The equation for the spin-dependent effective electron-electron interaction in three-dimensional electron gas was derived in the local mean field approximation by Kukkonen and Overhauser (KO) [1] and was made quantitative using local field factors from quantum Monte Carlo calculations by Kukkonen and Chen [2]. The effective electron-electron interaction in a deformable background is given by

$$V_{e\bar{\sigma}_1, e\bar{\sigma}_2} = \frac{4\pi e^2}{q^2} \left( \frac{1 + (1 - G_+)G_+Q}{1 + (1 - G_+)Q} - \frac{G_-^2 Q}{1 - G_-Q} \bar{\sigma}_1 \cdot \bar{\sigma}_2 \right) + \frac{1}{\omega^2 - \omega_q^2} \left( \frac{4\pi Ze^2}{q^2} \frac{1}{1 + (1 - G_+)Q} \right)^2 \frac{Nq^2}{M}. \quad (1)$$

This is the interaction to be used for calculating matrix elements between two electrons with moment  $k_1$  and  $k_2 = k_1 + q$  and spins  $\sigma_1$  and  $\sigma_2$ , differing in energy  $\hbar\omega$ . The density local field factor  $G_+$  and the spin local field factor  $G_-$  are wave vector and frequency dependent and the static local field factors are quantitatively given in Ref. [2]. The local field factors depend on the electron density  $n$  which is characterized by  $r_s (n = 4\pi (r_s a_0)^3 / 3)$ , where  $a_0$  is the Bohr radius.  $Q = v\Pi^0$ , where  $v$  is the Coulomb interaction  $v = 4\pi e^2 / q^2$  and  $\Pi^0$  is the Lindhard function. The wave vector and frequency dependence will not be indicated unless necessary. The word effective should be understood when discussing all of the interactions.  $N$  is the density and  $M$  is the mass

of the background (ions),  $Ze$  is their charge, and  $\omega_q$  is the dispersion relation of longitudinal excitations (phonons) of the background. For the derivation of Eq. (1), see Sec. VII of Refs. [2,3]. Equation (1) is based on linear response and mean-field theory, which have limitations but incorporate the essential physics of electrons in the uniform electron gas including exchange and correlation, as well as the screening effects of the deformable background (phonons).

The first term is the same as the electron-electron interaction in a rigid background. It is purely repulsive at low frequencies. For electrons with opposite spins, the dot product is negative and the spin-dependent term adds to the repulsion. For electrons with the same spin, the dot product is positive and the electron-electron interaction is less repulsive. For electrons with the same spins, the wave functions must be properly antisymmetric. This term is completely specified by the electron density and both local field factors.

The second term, which is attractive for  $\omega < \omega_q$ , results from additional screening by the deformable background. The quantity in parentheses is simply the electron-test charge interaction. While both local field factors appear in the spin-dependent first term in parentheses, this term depends only on the electron density, the density local field factor, and on the characteristics of the deformable background.

The form of Eq. (1) is exactly the same used by Pines [4] and many others subsequently to calculate the superconducting transition temperature for BCS superconductivity. The difference is that the electron-electron and the electron-test charge interactions in Eq. (1) include the effects of exchange and correlation, and that the deformable lattice screening was derived simply from an elastic medium without explicitly introducing phonons. Setting both local field factors to

<sup>\*</sup>kukkonen@cox.net

zero yields the Lindhard interaction or random phase approximation (RPA) interaction, which Pines approximated by the Thomas-Fermi interaction where the electron-electron, electron-test charge, and test charge-test charge interactions are all the same. In this case, Eq. (1) is identical to that used by Pines. A Fermi surface average of the repulsive electron-electron term for opposite spins became known as the superconducting parameter  $\mu$ , and the average of the attractive second term due to the deformable background (phonons) became  $\lambda$ . The goal was to be able to calculate the superconducting transition temperature based on properties of the normal metal.

Morel and Anderson [5] recognized that the Coulomb potential was essentially instantaneous and electrons moved at the Fermi velocity, while the deformable background had a much smaller speed of sound. This meant that the interaction between the two electrons in a Cooper pair was retarded in time. Morel and Anderson used an approximate solution to the Eliashberg equations [6] to capture this effect, and this led to a renormalized less repulsive interaction  $\mu^*$  which depends on  $\mu$  and the ratio of the Fermi temperature to the Debye temperature.

McMillan [7] anticipated that “given certain properties of the normal state of a given metal, we could calculate its superconducting properties, e.g.,  $T_c$ , with an accuracy of 1%.” McMillan approximately solved the Eliashberg equations for strong coupling, incorporated  $\mu^*$ , and fitted his result to known superconductors at the time and developed the famous McMillan formula Eq. (4) for the transition temperature, which depends only on normal state properties  $\mu^*$  and  $\lambda$ . Eliashberg theory has been the cornerstone of phonon-mediated superconductivity theory and has been recently reviewed by Marsiglio [8]. It is far beyond the limited scope of this paper.

Morel and Anderson and McMillan (and many others at the time) developed their theories based on the Thomas-Fermi approximation or the RPA, which treat all screened interactions identically. This gives the correct notional physics but, as these authors recognized, it is necessary to use the correct interactions in a quantitative theory. The correct interactions for the uniform electron gas were not available at that time, but are quantitatively available now and discussed in the Appendix.

Early calculations on superconductivity were done using the semiclassical Thomas-Fermi theory partly because the required integrals can be done analytically. The quantum Lindhard approximation, also known as the RPA, has been used extensively as well. The Thomas-Fermi and RPA are very close to each other, as shown in Fig. 10 in the Appendix. Neither include the effects of exchange and correlation. In this paper, the superconducting parameters calculated with the Thomas-Fermi interaction are compared to those using the correct electron-electron and electron-test charge interactions which include exchange and correlation. The comparisons using the RPA are essentially the same, and the same conclusions hold. This will show the quantitative effects on the superconducting parameters and the resulting calculated transition temperature using the McMillan formula. There is no serious attempt to compare with experiment and no consideration of effective masses, background dielectric constants,

quasiparticle renormalization or other factors that are required for comparison with experiments.

Density functional theory has been elaborated to include superconductivity, and this technique has been used extensively to calculate superconductivity in unique materials [9,10]. The density local field factor  $G_+$  is an input to these calculations which is sufficient to calculate the test charge-test charge and electron-test charge interactions needed for calculations of phonon spectra.

An *ab initio* Eliashberg theory was developed to incorporate full-scale Coulomb interactions from first principles [11] into superconducting density functional theory, thus avoiding any free parameters like  $\mu^*$ . The RPA was used to calculate electron-electron matrix elements. The author of this paper has contacted the lead author of Ref. [11], who has now used the KO interaction in the Eliashberg approach. The predicted superconducting transition temperature is reduced compared to the RPA as found in this paper, and full results will be reported in a subsequent publication.

The local field factors are crucial for quantitative calculations, and they have been studied for many years. Their behavior at small and large wave vectors are fixed by sum rules and there have been many attempts to quantify them [2,12–14]. Quantum Monte Carlo calculations are considered the best source of wave-vector dependence for the static local field factors [2,14]. The frequency dependence of the local field factors has been considered only rarely [12,13] and is usually ignored.

At the opposite extreme of superconductivity at low temperatures, there have been recent path integral Monte Carlo calculations of the uniform electron gas at temperatures near the Fermi temperature and above, which are applicable to warm dense matter [15,16]. The density local field factor has been calculated as a function of temperature, and used to calculate the effective potential between two electrons. The authors conclude that results predicted by the KO effective potential [Eq. (1)] are accurate and that the path integral Monte Carlo results constitute a small improvement.

The KO effective electron-electron interaction [Eq. (1)] was derived simply and intuitively. The local field factors in Ref. [2] are also very simple and quite accurate for wave vectors up to  $2k_F$ . These are used in all the calculations below. More accurate local field factors should be used if the calculations require wave vectors above  $2k_F$ .

To use Eq. (1) for the electron-proton gas, the equilibrium density  $r_s$  and the dispersion relationship  $\omega_q$  are needed. At small  $q$ , the dispersion relationship is determined by the bulk modulus  $B$  as discussed in Ref. [2]:

$$\omega_q^2 = \frac{Bq^2}{NM}. \quad (2)$$

The bulk modulus is taken from experimental data for the known metals.

Section II briefly presents the results of early work on calculating the superconducting transition temperature and shows how the electron-electron interaction in the normal state is used to predict superconductivity.

The repulsive superconducting parameters  $\mu$  and  $\mu^*$  are calculated in Sec. III using both KO and Thomas-Fermi interactions. The attractive parameter  $\lambda$  is calculated in Sec. IV

using three identical phonon dispersion relations to show the difference between  $\lambda$  calculated with the correct electron-test charge interaction and the Thomas-Fermi interaction. The sensitivity of the transition temperature calculated using the McMillan formula to these changes in  $\mu^*$  and  $\lambda$  are discussed in Sec. V.

Section VI discusses the results and points out the limitations of the simple model for the phonons used in this paper. The alkali metals are used as an example and current results are compared to other calculations.

## II. THE EFFECTIVE ELECTRON-ELECTRON INTERACTION AND SUPERCONDUCTIVITY

In 1958, shortly after the BCS theory was published, Pines [4] calculated the quantity  $N_0V$  that appears in the exponent for the transition temperature in the weak coupling limit and

$$T_c = 0.85 \Theta_D \exp\left(-\frac{1}{N_0V}\right). \quad (3)$$

$V$  is the sum of the electron-electron repulsion and the attractive term due to the phonons in the normal state averaged over the Fermi surface,  $N_0$  is the electronic density of states at the Fermi surface, and  $\Theta_D$  is the Debye temperature. This formula was used by Ashcroft [17] in his seminal paper on superconductivity in metallic hydrogen. Note that Pines considered the static interaction ( $\omega = 0$ ) and defined  $V$  with a minus sign compared to the convention used here.

The KO interaction was not available to Pines, and he used the Thomas-Fermi interaction for all screened Coulomb interactions. Pines used the Bohm-Staver [18] sound speed for noninteracting electrons, a Debye model for the phonons for wave vectors up to the Debye wave vector, and a different approximation to reflect umklapp scattering from the Debye wave vector to  $2k_F$ .

The Pines approach is simple and intuitive. Pines specified the average over the Fermi surface, which is simple for the spherical symmetry which he assumed and we follow. The average of the repulsive term has become known as the superconducting parameter  $\mu$  and the average of the attractive term is  $\lambda$ .

Hundreds of papers followed BCS and Pines. The two main and parallel goals of early research were to derive BCS theory using more formal many-body techniques, and also to apply the theory to the many metals that exhibited superconductivity. The simple connection  $N_0V = (\lambda - \mu)$  of Pines evolved to become the McMillan formula.

McMillan [7] considered the strong coupling limit and fitted  $T_c$  to an analytic function in terms of coupling constants  $\lambda$  and  $\mu^*$ . The resulting formula is

$$T_c = \frac{\Theta_D}{1.45} \exp\left(\frac{-1.04(1 + \lambda)}{\lambda - \mu^*(1 - 0.62\lambda)}\right). \quad (4)$$

$\mu^*$  was introduced by Morel and Anderson [5] to account for retardation and is given by

$$\mu^* = \frac{\mu}{1 + \mu \ln\left(\frac{T_F}{\Theta_D}\right)}, \quad (5)$$

where  $T_F$  is the Fermi temperature.

The McMillan formula was derived to fit the large group of then-known superconducting metals and alloys.  $\mu^*$  was calculated using the Thomas-Fermi approximation for the electron-electron interaction and known Debye temperatures, and found to be insensitive to the particular metal, and was largely assumed to be a constant with a value about 0.1 for all metals. The focus became  $\lambda$  which requires knowledge of the phonon spectra, as well as the electron-test charge interaction.

Pines, Morel and Anderson, and McMillan used the Thomas-Fermi interaction for all the screened Coulomb interactions in their calculations. However, they recognized that more was needed. Morel and Anderson [5] stated that their work was “based on the assumption that the screening radius of the electron-ion interaction is the same as the screening radius of the direct coulomb interactions between electrons and may be estimated on the basis of the Thomas Fermi model. This assumption is very much open to doubt...” McMillan [7] stated the necessary properties of the normal state needed to calculate the superconducting transition temperature are “(a) the electron energy bands near the Fermi energy, (b) the phonon dispersion curves, (c) the fully dressed (screened) electron-phonon interaction matrix elements and (d) the fully dressed Coulomb interaction between electrons.”

Now that the local field factors are accurately known from quantum Monte Carlo calculations, the effect of exchange and correlation can be simply incorporated into all superconductivity calculations. The KO interaction, Eq. (1), is used to calculate  $\mu$  and  $\lambda$  (using a simple approximation for the phonons). The results are compared to the Thomas-Fermi and RPA approximations (which are very close to each other) and ignore exchange and correlation. The RPA is obtained by setting all the local field factors to zero in Eq. (1).

The field of superconductivity calculations has advanced considerably. An *ab initio* theory of superconductivity has been developed using the density functional formalism with diagrammatic many-body perturbation theory to construct approximate exchange correlation functionals [9,10]. They find “unprecedented agreement with experimental results” for elemental superconductors using the Thomas-Fermi approximation. Another paper [11] on “*Ab-initio* Eliashberg Theory ... takes into account the Coulomb interaction in a full energy-resolved fashion avoiding any free parameters like  $\mu^*$ ”. Using the Thomas-Fermi interaction, their calculations validate the McMillan value of  $\mu^* = 0.11$ . The effect of using a correct interaction instead of Thomas-Fermi in this approach is unknown.

## III. REPULSIVE SUPERCONDUCTING PARAMETER $\mu$

Exchange and correlation in the electron gas make the repulsive electron-electron interaction stronger than the Thomas-Fermi interaction  $V_{TF}$ , and this inhibits superconductivity. The quantum mechanical version of the semiclassical Thomas-Fermi interaction is the Lindhard interaction, also known as the RPA,  $V_{RPA}$ . They are identical at  $q = 0$ , nearly the same at finite  $q$ , and are compared for  $r_s = 3.25$  in the Appendix. The superconducting parameter  $\mu$  is the average over the Fermi surface which is simply the density of states multiplied by the integral of the electron-electron interaction times  $q/(2k_F)^2$  from 0 to  $2k_F$  [4]. The free electron

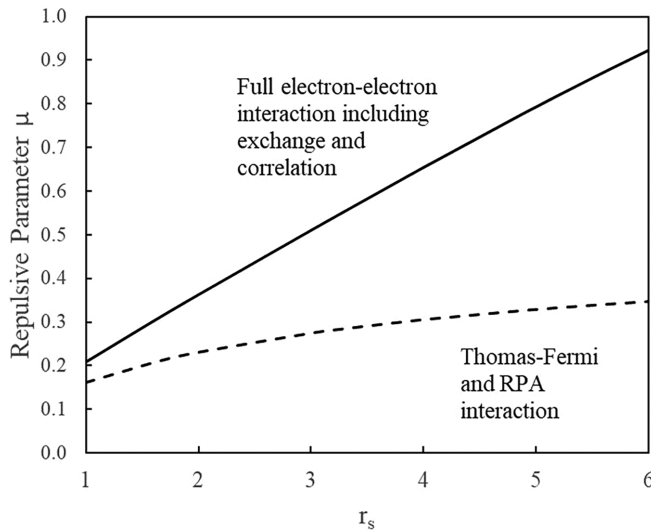


FIG. 1. Repulsive superconducting parameter  $\mu$  of the uniform electron gas including exchange and correlation compared to the value calculated using the Thomas-Fermi (with essentially the same results as the RPA interaction) as a function of  $r_s$ .

density of states for both spins is given by  $N_0 = m k_F / \hbar^2 \pi^2 = q_{TF}^2 / 4\pi e^2 = 1/V_{TF}(q=0)$ :

$$\mu = N_0 \int_0^{2k_F} \frac{q dq}{(2k_F)^2} V_{\uparrow\downarrow}(q). \quad (6)$$

For the uniform electron gas, the electron-electron interaction is completely specified by Eq. (1) and the local field factors given in Ref. [2]. The Thomas-Fermi interaction is also known, and the integrals are straightforward. The results are shown in Fig. 1.

The repulsive superconducting parameter  $\mu$  calculated with the KO electron-electron interaction given in Eq. (1) is much larger than the value calculated using the RPA and Thomas-Fermi interaction, and shown in Fig. 1. This is obvious because the correct electron-electron interaction is much larger than the RPA. See the Appendix for a specific example at  $r_s = 3.25$ .

To calculate  $\mu^*$  requires both the Fermi temperature and the Debye temperature which represents the phonons. The Fermi temperature was calculated at the density of the metals and the Debye temperature is given for representative elemental superconductors in Ref. [19] and for the alkali metals, most of which are not superconducting. The results are shown in Fig. 2. In a real metal, there is a background dielectric constant  $\epsilon_B$  and effective mass corrections due to band structure and many-body effects in the electron gas. The effective Bohr radius is given by  $a_B = \hbar^2 \epsilon_B / m e^2$ , and this determines the effective density of the electron gas in the metal. In addition, there may be other many-body effects such as the quasiparticle renormalization factor  $z_k$ . The present paper ignores all these effects. The intent is to show the difference in  $\mu^*$  when the effective electron-electron interaction is used rather than the Thomas-Fermi or RPA when other factors are held constant. The results are shown in Fig. 2.

The value of  $\mu^*$  calculated using the full electron-electron interaction shows the same trend as with the Thomas-Fermi interaction, but is only 20 – 25% larger. It has been previously

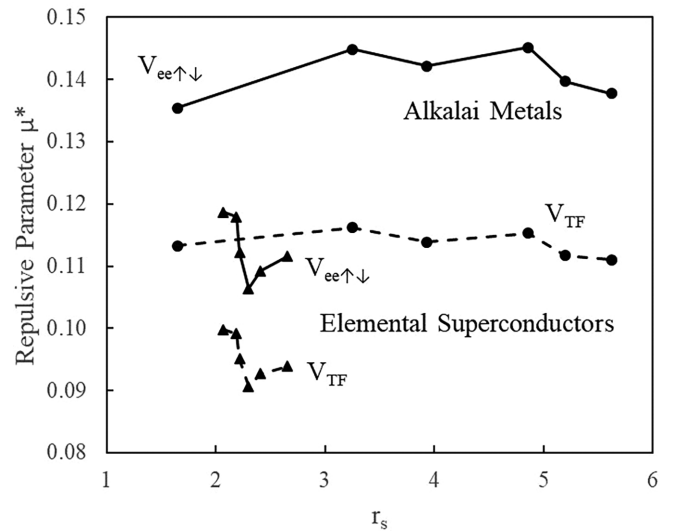


FIG. 2. Morel-Anderson effective repulsive parameter  $\mu^*$  calculated using the KO electron-electron interaction (solid line) compared to the Thomas-Fermi (or RPA) interaction (dashed line). The top data are calculated at the densities of the alkali metals: hydrogen, lithium, sodium, potassium, rubidium, and cesium. The lines between them are simply a guide to the eye. Representative elemental superconductors shown are aluminum, gallium, tin, lead, indium, and mercury in increasing order of  $r_s$ . There are no corrections for effective mass, dielectric background, or other factors. See text for further caveats. The input values for hydrogen  $r_s = 1.65$  are from the literature and discussed in Sec. V.

assumed that  $\mu^*$  was roughly a constant as a function of density with a value of 0.1, which simplified some analyses. The calculation of  $\mu^*$  for the alkali metals, which have more free-electron like behavior, is also shown because they have a larger range of  $r_s$ . For all the alkali metals  $\mu^*$  is nearly a constant with a value of  $\mu^* = 0.14 \pm 0.05$ .

The point of Figs. 1 and 2 is to show that both  $\mu$  and  $\mu^*$  differ substantially when calculated using the KO interaction that includes exchange and correlation compared to the RPA and Thomas-Fermi and RPA interactions that do not.

The sensitivity of the McMillan superconducting transition temperature to changes in  $\mu^*$  is shown in Fig. 3.

Figure 3 simply quantifies the changes that are obvious upon inspection of the McMillan equation. If  $\lambda$  is relatively small, the transition temperature is very sensitive to  $\mu^*$  and it is less sensitive for larger  $\lambda$ . Figure 2 shows that  $\mu^*$  is roughly 20% higher than the Thomas-Fermi value. This would lead to a 5 – 60% reduction in  $T_c$  predicted by the McMillan formula for a given value of  $\lambda$ . The difference is even larger compared to the often used constant value of  $\mu^* = 0.1$ .

#### IV. ATTRACTIVE SUPERCONDUCTING PARAMETER $\lambda$

In simple models, the attractive superconducting parameter  $\lambda$  is the same weighted average of the attractive part of the KO interaction given by the second term in Eq. (1) at  $\omega = 0$ :

$$\lambda = N_0 \int_0^{2k_F} \frac{q dq}{(2k_F)^2} V_{et}(q)^2 Z^2 \frac{N q^2}{M \omega_q^2}. \quad (7)$$



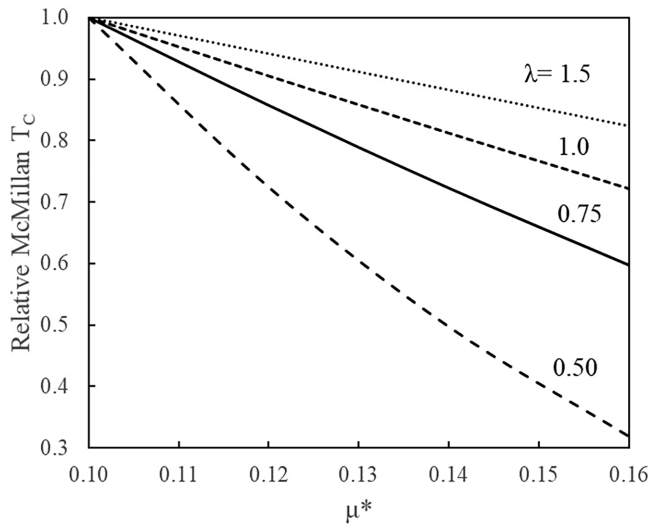


FIG. 3. Sensitivity of the superconducting transition temperature  $T_c$  to changes in the repulsive superconducting parameter  $\mu^*$  for given values of the attractive parameter  $\lambda$  using the McMillan formula.  $T_c$  is normalized to the value calculated for  $\mu^* = 0.1$ .

$ZV_{\text{et}}$  is the screened interaction between an electron and ion with charge  $Ze$  (see definition in the Appendix).

The expression for  $\lambda$  has two components, the electron-test charge interaction and the excitation spectrum  $\omega_q$ . This term is also known as the phonon propagator multiplied by the electron-phonon vertex [3]. The electron-phonon interaction and its use in calculations of superconductivity are reviewed in Ref. [20].

Although at  $q = 0$ , the electron-test charge interaction  $V_{\text{et}}$  is identically equal to the Thomas-Fermi and RPA interactions,  $V_{\text{et}}$  is larger at finite  $q$  and then converges above  $2k_F$ , which reflects the effects of exchange and correlation. This is shown in Fig. 10 in the Appendix. The effect on  $\lambda$  is even larger because the attractive term in Eq. (1) depends on  $V_{\text{et}}^2$ , which accentuates the difference.

Following Pines [4] and Seiden [21], a Debye model of the phonons [18] is employed. The small  $q$  (long wavelength) behavior is specified by the bulk modulus, but the  $q$  dependence at larger  $q$  must be approximated. The Debye wave vector  $k_D$  is the maximum phonon wave vector. It is determined by the density of ions  $N$  which is equal to the density of electrons ( $n$ ) divided by the number of electrons per ion  $Z$ ,  $N = n/Z = k_D^3/6\pi^2$ . Note that  $k_D = (2/Z)^{1/3}k_F$ , which equals  $1.26k_F$  for monovalent metals with  $Z = 1$ ,  $k_F$  for  $Z = 2$ ,  $0.87k_F$  for  $Z = 3$ , and  $0.79k_F$  for  $Z = 4$ . The Debye model has a linear dispersion  $\omega = (B/NM)^{1/2}q$ , where  $(B/NM)^{1/2}$  is the speed of sound. The maximum phonon frequency is at  $q = k_D$ , and the Debye temperature is defined as  $k_B\Theta_D = \hbar\omega_D = s k_D = \hbar(B/NM)^{1/2}k_D$ .

The maximum phonon wave vector for normal scattering for  $Z = 1$  is at  $q = k_D = 1.26k_F$ . Above  $q = 1.26k_F$ , there are phonons available that can scatter electrons, but they do not have a large enough wave vector to conserve momentum in the scattering. Pines [4] and Ashcroft [17] simply assumed there would be a mechanism for the ions or lattice to provide momentum as in umklapp scattering, and that the dispersion relation would remain constant above  $k_D$ .

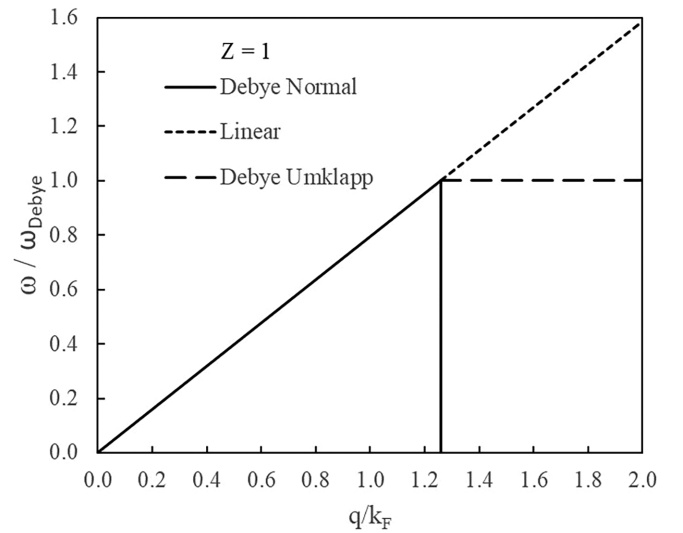


FIG. 4. Three simple dispersion relations based on the Debye model. The solid line with short dash extension assumes that there are phonons available to scatter electrons with momentum from zero to  $2k_F$ . The completely solid line represents the Debye model for normal scattering. The solid line with long dash extension recognizes that the highest energy phonon is at the Debye temperature, but that phonons can continue to scatter electrons with momentum conservation coming from the lattice (umklapp processes). This figure assumes  $Z = 1$ . The same approach is taken for different  $Z$  where  $k_D$  occurs at different values of  $q/k_F$  as discussed in the text.

Since  $\lambda$  is the integral of  $(V_{\text{et}}/\omega_q)^2$ , many different detailed structures of the phonon spectrum can yield the same  $\lambda$ . The goal is to compare the calculated  $\lambda$  using  $V_{\text{et}}$  and  $V_{\text{TF}}$  using exactly the same phonon dispersion relations. For this comparison, three simple dispersion relations are used. A simple completely linear dispersion relationship is given by  $\omega_q = sq$  for  $q = 0 - 2k_F$ , where  $s$  is the speed of sound. For normal scattering,  $\omega_q = sq$  for  $q = 0 - k_D$ . For normal plus umklapp scattering,  $\omega_q = sq$  for  $q = 0 - k_D$ , where  $k_D = (2/Z)^{1/3}$  is the Debye wave vector and  $\omega_q = s k_D$  for  $q = k_D - 2k_F$ . These are shown in Fig. 4 for an example where  $Z = 1$ .

Since the frequency squared appears in the denominator, the solid linear curve will predict a smaller  $\lambda$  than the dashed curve which is used to crudely model umklapp scattering. The linear curve should provide a weighting in the integral for  $\lambda$  that is an approximation to the worst case or smallest  $\lambda$ . The umklapp case is likely more realistic. Remember that the goal is not to accurately calculate  $\lambda$  but to show the importance of using the correct electron test charge interaction rather than the Thomas-Fermi or RPA interactions. These dispersion relations represent universal functions of  $q/k_F$  that scale directly with the Debye temperature  $\Theta_D$ , which is determined by the bulk modulus (or sound velocity). Therefore,  $\lambda$  is given by the ratio of the bulk modulus of the free electron gas to the actual bulk modulus times a universal function of  $r_s$  and  $Z$  which is completely determined by  $k_f$  and  $k_D$ :

$$\lambda = \frac{B_0}{B} \lambda_{\text{universal}} = \frac{B_0}{B} \left( \int_0^{k_D} \frac{q dq}{(2k_F)^2} V_{\text{et}}^2 + \int_{k_D}^{2k_F} \frac{q dq}{(2k_F)^2} V_{\text{et}}^2 \left( \frac{q}{k_D} \right)^2 \right). \quad (8)$$

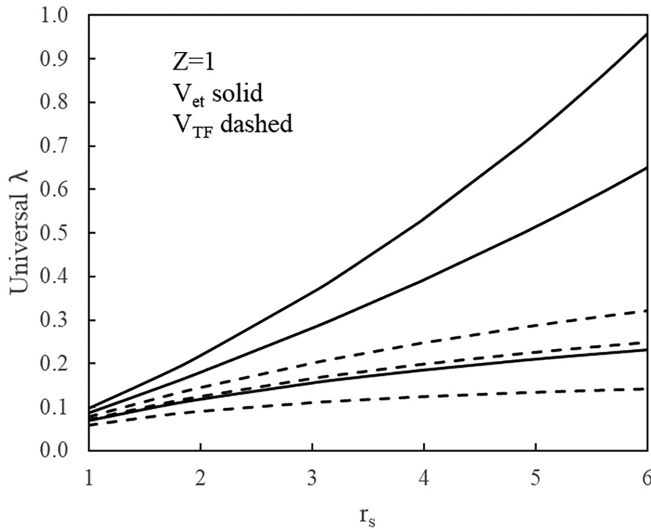


FIG. 5. Universal attractive superconducting parameter  $\lambda_{\text{universal}}$  from Eq. (8) for monovalent metals  $Z = 1$ . The results for the electron-test charge interaction  $V_{\text{et}}$  are compared to the Thomas-Fermi interaction for the three dispersion curves of Fig. 4. The top curve is for normal plus umklapp scattering, the middle curve for the linear dispersion relation, and the bottom curve is for normal scattering only.

As an example,  $\lambda_{\text{universal}}$  is plotted in Fig. 5 for  $Z = 1$  ( $k_D = 1.26 k_F$ ), where both the linear dispersion and umklapp dispersion relations are calculated using  $V_{\text{et}}$  and  $V_{\text{TF}}$ .

The curves using  $V_{\text{et}}$  are substantially higher than  $V_{\text{TF}}$ , and increasingly so as a function of  $r_s$ . The same curves were generated for  $Z = 1 - 4$  and the enhancement ratio  $\lambda_{\text{et}}/\lambda_{\text{TF}}$  is shown in Fig. 6.

Figure 6 shows that for the three phonon dispersion relations and different values of  $Z$ , the value of  $\lambda$  calculated using

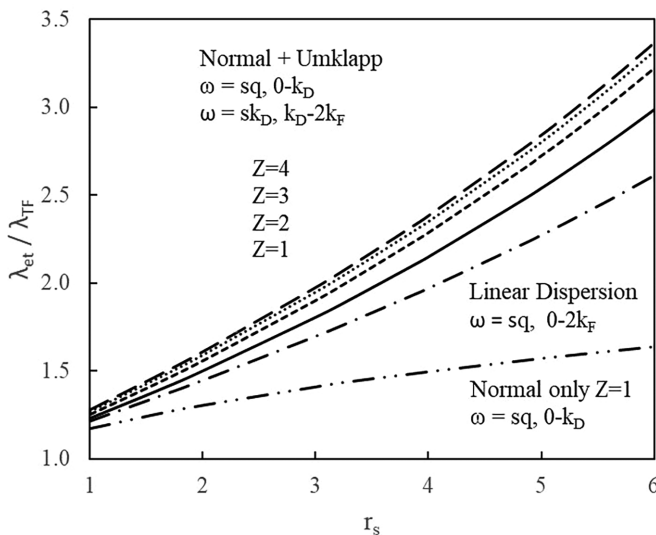


FIG. 6. Ratio of the attractive superconducting parameter  $\lambda$  calculating using the electron-test charge interaction  $V_{\text{et}}$  compared to those using the Thomas-Fermi interaction  $V_{\text{TF}}$ , which is very close to the RPA (Lindhard) interaction.

the electron-test charge interaction is substantially higher than that using the Thomas-Fermi interaction. Both interactions are identical at  $q = 0$ , but differ significantly at finite  $q$ . This clearly demonstrates the importance of using the correct interaction. Most superconducting metals have  $r_s$  between 2.07 and 3.25. In this model, the calculation of  $\lambda$  using  $V_{\text{et}}$  would be approximately 35% to 75% larger than that predicted by the Thomas-Fermi interaction.

Modern calculations of the phonon dispersion relations are performed using density functional theory. If the exchange-correlation kernel is correct, then the self-consistent potentials used to calculate the ion-ion and the electron-ion interactions needed should also be correct. In any case, the phonon dispersion relations can be compared to experiments. If the same self-consistent potential is used to calculate the electron-phonon matrix elements, then the value of  $\lambda$  should also be correct. This is more difficult to compare with experiments. If the Thomas-Fermi or RPA interactions are invoked at any stage, the results are probably quantitatively in error.

## V. IMPLICATIONS OF THE MCMILLAN EQUATION

McMillan [7] took the measured transition temperatures of metals and the Debye temperature, and extracted  $\lambda$  using an empirically derived value of  $\mu^*$  which he took to be 0.13 for the transition metals and 0.1 for nearly free electron metals. He and many others, previously and subsequently, attempted to calculate  $\lambda$  from first principles. Since  $T_c$  was known and  $\mu^*$  was assumed, the McMillan equation was solved for the empirical  $\lambda$ , which became the target for first-principles calculations. If the calculation of  $\lambda$  predicted the observed transition temperature, this validated the calculation. In the early days, all screened Coulomb interactions were treated simply as the bare Coulomb interaction divided by the dielectric function which was calculated in the Thomas-Fermi or RPA approximation. The focus was on the phonon dispersion relations of real metals that are needed to calculate  $\lambda$ .

Including exchange and correlation increases both  $\mu^*$  and  $\lambda$  significantly over the Thomas-Fermi or RPA approximations as shown above. To show the impact on the calculation of the superconducting transition temperature using the McMillan formula, it is plotted below in Fig. 7.

Figure 7 shows that the exponential part of the McMillan equation is roughly a linear function of  $\lambda$  for values of  $\mu^*$  and  $\lambda$  of interest to conventional superconductors. An example of the impact of using the KO interaction instead of the Thomas-Fermi interaction can be illustrated by considering a fictitious metal that had  $\mu^* = 0.1$  and  $\lambda = 0.8$  calculated using the Thomas-Fermi interaction. The McMillan equation would predict that  $T_c/(\Theta_D/1.45) = 0.056$ . Using the KO interaction would predict that  $\mu^* = 0.12$  and  $\lambda = 1.1$  for the same phonon dispersion curve. This would predict that  $T_c/(\Theta_D/1.45) = 0.088$  which is 57% higher. If for this fictitious metal,  $\lambda$  was calculated correctly using the self-consistent electron-test charge from density functional theory (which should be the same as  $V_{\text{et}}$ ) for the matrix elements, but used the Thomas-Fermi interaction to calculate  $\mu^* = 0.1$  instead of 0.12, the resulting transition temperature would be 13% lower. The difference in using the Thomas-Fermi interaction compared to the KO interaction is even more dramatic for

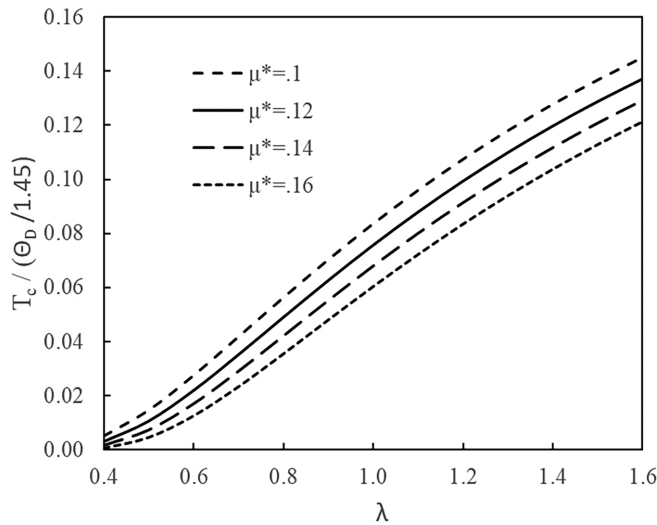


FIG. 7. The McMillan equation [Eq. (4)] plotted versus  $\lambda$  for four different values of  $\mu^*$ .

small  $\lambda$  where the McMillan equation is exponential. Over the years, different authors have suggested that the prefactor in the McMillan equation,  $\Theta_D/1.45$ , should be somewhat different. The conclusions above are independent of the prefactor.

In summary, using the KO interaction instead of the Thomas-Fermi or RPA interactions which ignore exchange and correlation has the effect of increasing the repulsive parameter  $\mu^*$  which inhibits superconductivity, but exchange and correlation also increases the attractive parameter  $\lambda$  which enhances superconductivity. The increase in  $\lambda$  is significantly larger than the increase in  $\mu^*$ , so the net predicted transition temperature would be substantially larger.

## VI. DISCUSSION AND LIMITATIONS

With quantitative knowledge of the uniform electron gas interactions and a simple Debye model for the phonons, the conducting parameters  $\mu$ ,  $\mu^*$ , and  $\lambda$  can be calculated with only the inputs of the electron density  $r_s$  and the bulk modulus (or, equivalently, the sound velocity). The bulk modulus can be measured or calculated, as can the Debye temperature.

The limitations of this model for the phonons become apparent when considering the alkali metals. The density ( $r_s$ ) and bulk modulus of each is known and the superconducting parameters can be calculated. Theorists have made extensive calculations on hydrogen. Ashcroft, in 1969, [17] originally suggested that hypothetical metallic hydrogen might exist at  $r_s$  about 1.6. He further calculated the compressibility, which is the inverse of the bulk modulus, and predicted that because of its light mass, the Debye temperature would be 3500 K. He first suggested that metallic hydrogen would be a high temperature superconductor. In 1987, Ceperley and Alder [22] performed quantum Monte Carlo calculations of the properties of solid hydrogen at high pressures. They found an atomic metallic phase and calculated the energy and pressure as a function of  $r_s$  for both bcc and fcc lattices. The energy minimum for was approximately  $r_s = 1.6-1.7$ . The bulk modulus can be estimated by differentiating the pressure curve. Both

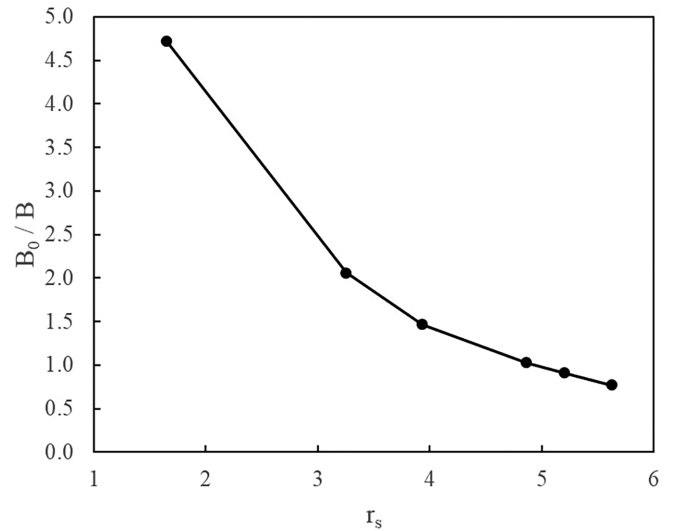


FIG. 8. Ratio of the free electron bulk modulus to the calculated value for the electron-proton gas and the measured values [23] for the other alkali metals at their densities. The solid line is simply a guide to the eye.

results are consistent with  $r_s = 1.65$  and  $B = 150$  GPa. This is also consistent with the Debye temperature of 3500 K. Figure 8 shows the ratio of the free electron bulk modulus to the measured [23] or calculated bulk modulus for hydrogen and the alkali metals.

Using these values, the superconducting parameters for this version of the hypothetical metallic hydrogen were calculated and are shown in Fig. 9, along with those of the known alkali metals.

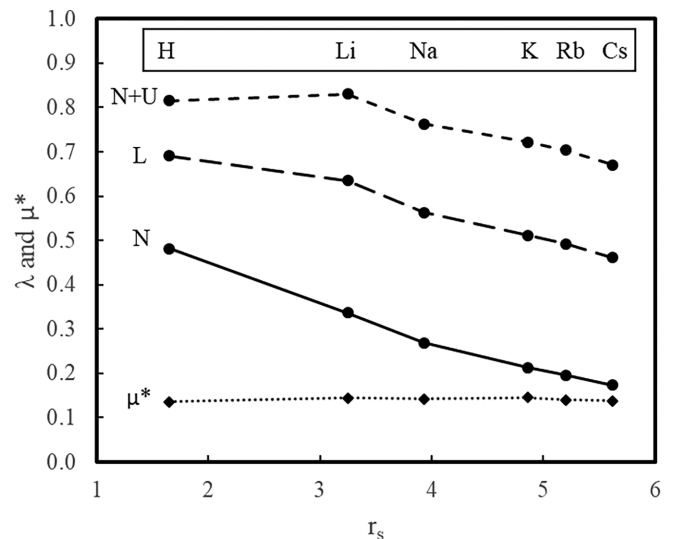


FIG. 9. The KO interaction [Eq. (1)] is used to calculate the repulsive superconducting parameter  $\mu^*$  as a function of  $r_s$ , the attractive superconducting parameter  $\lambda$  using the three simple model phonon dispersion relations shown in Fig. 4, and using the bulk moduli shown in Fig. 8. The lines are simply a guide to the eye.  $N$  is for normal scattering only without umklapp scattering,  $L$  is for a completely linear dispersion relationship, and  $N + U$  is for normal plus umklapp.

The repulsive parameter  $\mu^*$  in Fig. 9 is the same as shown in Fig. 2 and varies only slightly in the range 0.135–0.145 and is included for easy comparison to the attractive parameter  $\lambda$ . The values of  $\lambda$  in Fig. 9 are the product of the universal  $\lambda$  of Fig. 4 which increase with  $r_s$ , and the bulk modulus ratio  $B_0/B$  of Fig. 8 which decrease rapidly with  $r_s$ . The  $N + U$  values of  $\lambda$  might be expected to be most accurate.

The first conclusion of examining Fig. 9 is that  $\lambda - \mu^*$  is positive for all the alkali metals, which implies all of them should be superconducting. This is also true if the Thomas-Fermi approximation is used. Morel and Anderson noted this problem [5].

There has been considerable theoretical work on metallic hydrogen and lithium initially focusing on  $\lambda$ . Previous theoretical values of  $\lambda$  of metallic hydrogen ranged from 15–90% higher than  $\lambda$  for  $N + U = 0.815$  calculated here [24–26]. Using  $\lambda = 0.815$  and  $\mu^* = 0.135$  in the McMillan equation predicts a superconducting transition temperature of 105 K, which is quite high but lower than that of previous calculations.

Lithium is the only alkali metal that has exhibited superconductivity at ambient pressure. The transition temperature is very low:  $T_c = 0.4$  mK [27]. Detailed lithium calculations by Liu and Quong [28] found  $\lambda = 0.45$  and they concluded that  $\mu^* = 0.28$  was required in the McMillan formula to agree with experiment. Lithium was also examined using density functional theory extended to the superconducting state [29]. They found  $\lambda = 0.38$  and that  $\mu^* = 0.23$  was required to achieve agreement with their results at all pressures. Richardson and Ashcroft [30] found that  $\mu^* = 0.237$  was required. These values of  $\lambda$  are lower than calculated here for  $N + U$ , whereas  $\mu^*$  is much higher. Note again that the current calculations do not consider effective mass, background dielectric constant, renormalization factors, etc.

It is clear from examining the Morel and Anderson equation for  $\mu^*$  [Eq. (5)] that the above values of  $\mu^*$  are not possible for any plausible values of  $\mu$  or  $\Theta_D$ . Akashi and Arita [31] calculated that plasma assisted phonon scattering could explain the data for lithium. The authors of Ref. [32] found that “the suppression of the critical temperature is entirely due to the re-normalized Fermi liquid properties” and “conclude that the original interpretation of  $\mu^*$  by Morel and Anderson is incorrect and misleading.” They also state that “Our results call for radical reconsideration of the widely accepted picture that the effect of Coulomb interactions reduces to a (weak) repulsive pseudo-potential.”

It appears that there remain unresolved issues in the pursuit of quantitative predictions of the superconducting transition temperature using the BCS theory, the Morel and Anderson  $\mu^*$ , and the McMillan equation.

## VII. CONCLUSIONS

The primary goal of this paper is to compare calculations of the superconducting parameters  $\mu$  and  $\lambda$  using electron-electron and electron-test charge interactions that include exchange and correlation through local field factors to the same calculations using the Thomas-Fermi (and nearly equivalent RPA) interaction. The KO interaction, Eq. (1), which depends on  $r_s$  and both the density local field factor  $G_+$  and

the spin local field factor  $G_-$ , is used to calculate  $\mu$ , which is found to be substantially larger than the Thomas-Fermi result. The differences are reduced when using the Morel Anderson  $\mu^*$ , which depends also on the Debye temperature. In typical cases, the KO interaction increases  $\mu^*$  by about 20% over the Thomas-Fermi result. Using the McMillan formula, this results in a 5–60% lower predicted superconducting transition temperature, depending on the value of  $\lambda$ .

The attractive superconducting parameter  $\lambda$  depends both on the phonon spectrum and the electron-test charge (electron-phonon) matrix elements. Both of these elements require only the density local field factor  $G_+$ . Early investigators used the Thomas-Fermi interaction, which ignores the exchange and correlation ( $G_+ = 0$ ) instead of  $V_{et}$ . Both are the same at  $q = 0$ , but  $V_{et}$  is substantially larger at larger  $q$ , which is the region of greatest weight when averaging over the Fermi surface. The correct value of  $\lambda$  is 35–75% or more larger than that calculated with the Thomas-Fermi interaction. Most modern calculations of  $\lambda$  use density functional theory. If the exchange and correlation kernel used is correct, and the matrix elements are calculated using the self-consistent potential, these calculations of  $\lambda$  should be accurate.

The conclusion is that calculations using the Thomas-Fermi (or RPA) interaction may yield qualitative results, but not quantitative results for superconductivity properties. The local field factors are quite well-known and simple to apply, so there is no reason to make other approximations such as Thomas-Fermi or RPA.

## ACKNOWLEDGMENTS

The author appreciates technical discussions with Jan Herbst and his careful reading of the paper. Daniel Arturo Brito Urbina provided computational assistance and prepared the publication version of the paper.

## APPENDIX: QUANTITATIVE EVALUATION OF DIFFERENT INTERACTIONS IN THE UNIFORM ELECTRON GAS

The Thomas-Fermi and RPA/Lindhard interactions were used to represent screened interactions for many years before the effects of exchange and correlation were well-known. They are sometimes used even today because they are simple. This Appendix is intended for nonexperts to illustrate the substantial quantitative difference between these interactions and the correct interactions that incorporate exchange and correlation.

It is now well established that the interactions between two test charges (ions or protons), an electron and a test charge, between two electrons of opposite spins, and two electrons with parallel spins are all different.

A Coulomb charge introduced into the electron gas induces a screening cloud of opposite charge that creates an additional electric potential that reduces the bare Coulomb potential from the original charge. This electric potential is what is felt by another test charge and defines the dielectric function. An electron interacting with an external charge also feels the Coulomb potential but has additional interactions with the screening cloud because the electron is identical to the same



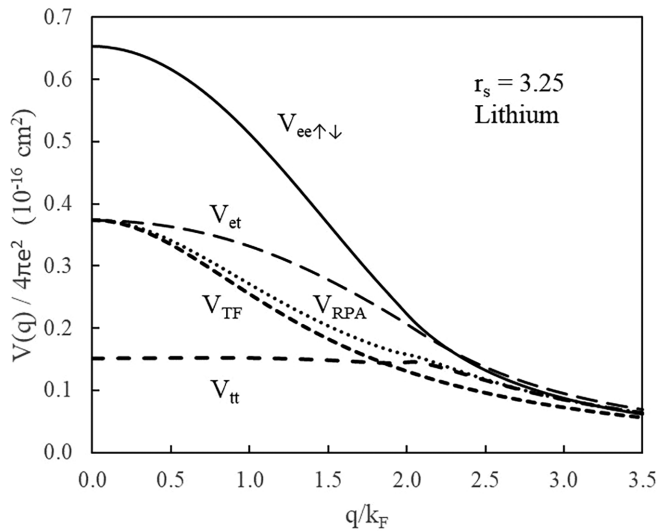


FIG. 10. Interactions in the electron gas including exchange and correlation are compared to the Lindhard/RPA and Thomas-Fermi interactions at  $r_s = 3.25$ , which is the density of lithium.  $V_{ee\uparrow\downarrow}$  is the interaction between two electrons of opposite spin.  $V_{et}$  is the interaction between an electron and a test charge.  $V_{tt}$  is the screened Coulomb interaction between two test charges.

spin electrons in the screening cloud and has an exchange interaction with them. This introduces a vertex correction. Of course, the electrons in the screening cloud have exchange interactions with each other and they also repel each other through their Coulomb interaction, which is called correlation. For the interaction between two test charges  $V_{tt}$ , exchange and correlation only occur in the interactions among the electrons in the screening cloud, which are expressed in the dielectric function. The interaction between the electron and a test charge (ion or proton)  $V_{et}$  includes the dielectric function, but the electron under consideration also has exchange and correlation interactions with the induced screening charge and requires a vertex correction. The electron-electron interaction  $V_{ee}$  is different again, because both the electrons have exchange and correlation interactions. Furthermore, if the two electrons have parallel spins, they can exchange with each other as well as with the screening cloud. Therefore,  $V_{ee}$  is spin dependent and  $V_{ee\uparrow\downarrow}$  for opposite spins is more repulsive than  $V_{ee\uparrow\uparrow}$  for parallel spins.

These different interactions are discussed in detail in Ref. [2]. For superconductivity, the BCS interaction is between antiparallel spins [the dot product in Eq. (1) is +1 for antiparallel spins and  $-1$  for parallel spins].

For completeness and for easy comparison, the well-known forms for the test charge-test charge and electron test charge interactions including exchange and correlation are given:

$$V_{tt} = \frac{V_{\text{ext}}}{\varepsilon}, \quad (\text{A1})$$

$$V_{et} = \frac{\Lambda V_{\text{ext}}}{\varepsilon}. \quad (\text{A2})$$

$\Lambda$  is the vertex correction and  $\varepsilon$  is the dielectric function:

$$\Lambda = \frac{1}{1 - G_+ Q}, \quad (\text{A3})$$

$$\varepsilon = 1 + \Lambda Q. \quad (\text{A4})$$

Note that  $\Lambda/\varepsilon = 1/(1 + Q(1 - G_+))$ .

The density local field factor  $G_+$  incorporates the effects of exchange and correlation. Simple and quite accurate approximations to  $G_+(q)$  and  $G_-(q)$  are given in Ref. [2]. Setting  $G_+ = 0$ , all the interactions are equal to the Lindhard/RPA interaction. The Thomas-Fermi interaction is obtained by replacing the Lindhard function by its  $q = 0$  value. To quantitatively illustrate the effect of exchange and correlation, all these interactions are evaluated and compared in Fig. 10 below for a representative density of  $r_s = 3.25$  appropriate for lithium.

Figure 10 illustrates the well-known differences amongst these interactions. The Thomas-Fermi interaction was derived semiclassically and the Lindhard/RPA interaction includes quantum Fermi statistics, but does not include exchange and correlation. At very high density,  $r_s \ll 1$ , the kinetic energy of the electron gas dominates the effects of exchange and correlation, the Lindhard/RPA interaction is accurate, and all of the interactions tend toward this limit. However, at the densities of metals, the exchange and correlation cannot be ignored and the correct interactions must be used to make quantitative predictions. The electron-test charge interaction is equal to Lindhard/RPA and Thomas-Fermi at  $q = 0$ , but deviates significantly at intermediate wave vector. All the interactions converge at a large wave vector, reflecting the fact that screening is ineffective at very short distances.

Since the local field factors are well-known with simple approximations for the uniform electron gas, the correct interactions including exchange and correlation should be used for all calculations. This is well recognized for time-dependent density functional theory where exchange and correlation is routinely used. However, perturbation theory and superconductivity calculations still sometimes use the RPA.

- [1] C. A. Kukkonen and A. W. Overhauser, *Phys. Rev. B* **20**, 550 (1979).
- [2] C. A. Kukkonen and K. Chen, *Phys. Rev. B* **104**, 195142 (2021).
- [3] G. Giuliani and G. Vignale, *Quantum Theory of the Electron Liquid* (Cambridge University Press, Cambridge, England, 2005).
- [4] D. Pines, *Phys. Rev.* **109**, 280 (1958).
- [5] P. Morel and P. Anderson, *Phys. Rev.* **125**, 1263 (1962).

- [6] G. Eliashberg, *Sov. Phys. JETP* **11**, 696 (1960).
- [7] W. McMillan, *Phys. Rev.* **167**, 331 (1968).
- [8] F. Marsiglio, *Ann. Phys.* **417**, 168102 (2020).
- [9] M. Lüders, M. A. L. Marques, N. N. Lathiotakis, A. Floris, G. Profeta, L. Fast, A. Continenza, S. Massidda, and E. K. U. Gross, *Phys. Rev. B* **72**, 024545 (2005).
- [10] M. A. L. Marques, M. Lüders, N. N. Lathiotakis, G. Profeta, A. Floris, L. Fast, A. Continenza, E. K. U. Gross, and S. Massidda, *Phys. Rev. B* **72**, 024546 (2005).

- [11] A. Sanna, J. A. Flores-Livas, A. Davydov, G. Profeta, K. Dewhurst, S. Sharma, and E. Gross, *J. Phys. Soc. Jpn.* **87**, 041012 (2018).
- [12] C. F. Richardson and N. W. Ashcroft, *Phys. Rev. B* **50**, 8170 (1994).
- [13] A. Ruzsinszky, N. K. Nepal, J. M. Pitarke, and J. P. Perdew, *Phys. Rev. B* **101**, 245135 (2020).
- [14] S. Moroni, D. M. Ceperley, and G. Senatore, *Phys. Rev. Lett.* **75**, 689 (1995).
- [15] T. Dornheim, J. Vorberger, S. Groth, N. Hoffmann, Z. A. Moldabekov, and M. Bonitz, *J. Chem. Phys.* **151**, 194104 (2019).
- [16] T. Dornheim, P. Tolias, Z. A. Moldabekov, A. Cangi, and J. Vorberger, *J. Chem. Phys.* **156**, 244113 (2022).
- [17] N. W. Ashcroft, *Phys. Rev. Lett.* **21**, 1748 (1968).
- [18] N. W. Ashcroft and N. D. Mermin, *Solid State Physics* (Holt, Rinehart and Winston, New York, 1976).
- [19] K. Door, Debye temperature (2022), [https://www.knowledgedoor.com/2/elements\\_handbook/debye\\_temperature.html](https://www.knowledgedoor.com/2/elements_handbook/debye_temperature.html).
- [20] F. Giustino, *Rev. Mod. Phys.* **91**, 019901(E) (2019).
- [21] P. E. Seiden, *Phys. Rev.* **168**, 403 (1968).
- [22] D. M. Ceperley and B. J. Alder, *Phys. Rev. B* **39**, 2092 (1987).
- [23] P. Table, Technical data for cesium (2022), <https://periodictable.com/Elements/055/data.html>.
- [24] T. Schneider and E. Stoll, *Physica* **55**, 702 (1971).
- [25] T. Barbee, A. García, and M. L. Cohen, *Nature (London)* **340**, 369 (1989).
- [26] C. F. Richardson and N. W. Ashcroft, *Phys. Rev. Lett.* **78**, 118 (1997).
- [27] J. Tuoriniemi, K. Juntunen-Nurmilaukas, J. Uusvuori, E. Pentti, A. Salmela, and A. Sebedash, *Nature (London)* **447**, 187 (2007).
- [28] A. Y. Liu and A. A. Quong, *Phys. Rev. B* **53**, R7575 (1996).
- [29] G. Profeta, C. Franchini, N. N. Lathiotakis, A. Floris, A. Sanna, M. A. L. Marques, M. Lüders, S. Massidda, E. K. U. Gross, and A. Continenza, *Phys. Rev. Lett.* **96**, 047003 (2006).
- [30] C. F. Richardson and N. W. Ashcroft, *Phys. Rev. B* **55**, 15130 (1997).
- [31] R. Akashi and R. Arita, *J. Phys. Soc. Jpn.* **83**, 061016 (2014).
- [32] T. Wang, X. Cai, K. Chen, B. V. Svistunov, and N. V. Prokof'ev, [arXiv:2207.05238](https://arxiv.org/abs/2207.05238).